Electrochemistry Communications 65 (2016) 48–52

Contents lists available at ScienceDirect

Electrochemistry Communications

journal homepage: www.elsevier.com/locate/elecom

A theoretical model to determine intercalation entropy and enthalpy: Application to lithium/graphite

Eduardo M. Perassi *, Ezequiel P.M. Leiva *

Instituto de Investigaciones en Fisicoquímica de Córdoba (INFIQC), Dpto. de Matemática y Física, Facultad de Ciencias Químicas, Universidad Nacional de Córdoba, Córdoba, Argentina

ARTICLE INFO

Article history:
Received 30 December 2015
Received in revised form 4 February 2016
Accepted 5 February 2016
Available online 16 February 2016

Keywords:
Entropy
Intercalation
Lithium-ion battery
Lattice-gas
Monte Carlo
Graphite

ABSTRACT

Intercalation compounds play a fundamental role to increase the capabilities of electrochemical cells to store energy. A new computational model is developed to calculate the intercalation entropy and enthalpy in electrochemical intercalation compounds. The new methodology is applied to the intercalation of lithium ions into graphite, finding a good agreement with experimental measurements. The main features of the experimental data are correctly reproduced, including the step in the intercalation entropy and enthalpy for the stage II to stage I transition.

1. Introduction

In recent years, measurements of open-circuit voltage (OCV) at different temperatures of an electrochemical cell upon energy storage have been used to characterize the intercalation entropy and enthalpy of the cell [1,2,3,4]. These measurements are performed by changing the temperature of the cell and measuring the equilibrium value of the OCV for the new temperature. The OCV vs. temperature measurements are collected for different states of charge of the electrodes of the cell. Since the OCV vs. temperature measurements are time-consuming as it is necessary to reach the equilibrium value of the OCV, different methods to measure the intercalation entropy have been recently developed [5,6].

The continuing and increasing new developments of batteries of electrochemical cells to store energy require of new and more sophisticated parameters to characterize and optimize their performance. The intercalation entropy is one of them and constitutes a very important thermodynamic value as it allows us to analyze the reversible heat generation in the electrode materials of a battery. When the battery size increases the area-to-volume ratio decreases and the heat transfer away from the battery becomes more inefficient [7,8]. The total heat generation rate can be divided into reversible and irreversible parts. The irreversible part depends on the internal resistance of the cells whereas the reversible one is a function of the intercalation entropy [9,8]. It was found that the reversible heat generation rate is a significant portion of the total heat generation rate and that it can contribute to more than 50% of the total generated heat at the C/1 discharge rate [10,11,8]. Therefore, it is very important to determine the intercalation entropy of an electrochemical cell to prevent high temperature excursions of their electrode materials.

In the last years and accompanying the developing of cells to store energy, different theoretical approaches have been applied to understand and improve the performance of anodic and cathodic materials. In this sense, insertion and intercalation potentials for different electrode materials were determined by means of *ab initio* methods [12, 13,13,14,15]. Diffusion barriers were obtained from *ab initio* and quantum Monte Carlo [16,17,18] calculations. Molecular dynamic simulations have been used in diffusion studies [19,20,21]. Intercalation studies of ions were performed by mean of a lattice-gas model by using the mean-field approximation and Monte Carlo simulations [22, 23]. In recent times multiscale physical models have emerged, spanning scales from few atoms to the device level that can predict the behavior of the materials and their time evolution. These methods, subject of different extensive reviews [24,25,26] may profit from the previous fine grained methods, using some of their results as input.

Here we show how the intercalation entropy and enthalpy can be theoretically determined. As previously stated some of the outputs of the present theoretical model like the intercalation entropy may be useful for multiscale models [26]. Particularly, we study the *Li*_graphite intercalation compound by modeling it as a lattice-gas and performing grand

* Corresponding authors.
E-mail addresses: eduardo.perassi@gmail.com (E.M. Perassi), eze_leiva@yahoo.com.ar (E.P.M. Leiva).

http://dx.doi.org/10.1016/j.elecom.2016.02.003
1388-2481/

canonical Monte Carlo simulations. The main features of the experimental intercalation entropy and enthalpy are correctly reproduced.

2. Material and methods

Reynier et al. have experimentally studied the intercalation entropy and enthalpy of *Li*-ions into graphite by using test half-cells with metallic lithium as counter and reference electrodes and a composite graphite working electrode [1]. The theoretical results of the present work are compared below with experimental data of OCV, intercalation entropy and enthalpy vs. lithium concentration (x), which were picked up from the work of Reynier et al. [1].

3. Theory and computational methods

To calculate the intercalation entropy of intercalation compounds, a lattice gas model is considered within a grand canonical ensemble, where the volume of the system is constant and the particle number may change. The total energy of the system is given by:

$$U(S,V,N) \tag{1}$$

where S is the entropy, V is the volume and N the number of particles of the system. An increment of the energy is given by:

$$dU = TdS + PdV + \mu \mathrm{dN} \tag{2}$$

where T is the temperature and μ is the chemical potential. The constant volume condition in our model yields:

$$dU = TdS + \mu \mathrm{dN} \tag{3}$$

Therefore, the intercalation entropy is given by:

$$\frac{dS}{dN} = \frac{1}{T}\left(\frac{dU}{dN} - \mu\right) \tag{4}$$

For a given T and μ a Monte Carlo grand canonical simulation is performed and the energy change ΔU is calculated and saved for each accepted particle insertion or deletion in the simulation. In this way the following mean value is obtained:

$$<\frac{dU}{dN}> = \frac{\Sigma_i^{N_i}\Delta U_i - \Sigma_d^{N_d}\Delta U_d}{N_i + N_d} \tag{5}$$

where i and d denote insertion and deletion moves respectively. Finally, the mean value of the intercalation entropy is obtained from:

$$\frac{dS}{dN} = \frac{1}{T}\left(<\frac{dU}{dN}> - \mu\right) \tag{6}$$

Seeking for a particular application of the above formalism, a lattice-gas model is employed to study the insertion of *Li*-ions into graphite. The centers of the carbon hexagons in a graphite with AA stacking [27,28,29] are used to define the lattice for the *Li*-ion gas. The sites of the lattice are located at a distance d from these centers. This distance corresponds to half of the distance between the (0001) graphite basal planes. Fig. 1a shows a top view of a *Li*-ion (green) on a lattice site and Fig. 1b shows a lateral view of this *Li*-ion.

The interactions between the ions of the gas are divided into two parts, the in-plane interactions and the out-of-plane interactions. The in-plane interactions are the interactions between ions in the same layer of graphite. These interactions are assumed to be given by a Lennard-Jones potential [30,31]:

$$V_{ij} = c_i c_j \in \left[\left(\frac{r_m}{r_{ij}}\right)^{12} - 2\left(\frac{r_m}{r_{ij}}\right)^{6}\right] \tag{7}$$

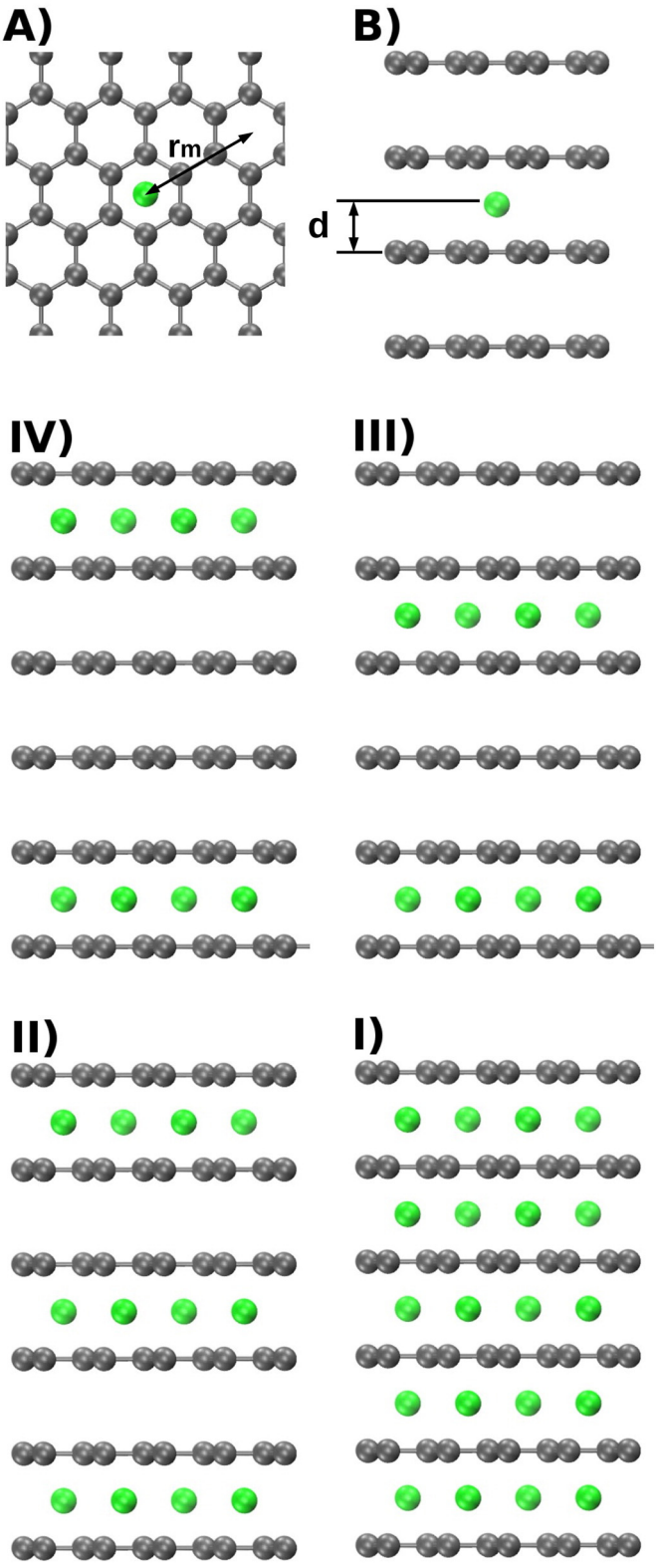

Fig. 1. A) Scheme of a top view of a *Li*-ion (green) on a lattice site. The distance to the second neighbor r_m is also indicated. B) A lateral view of the *Li*-ion on the lattice site. IV-I) Schemes of four known stages of the *Li*-graphite intercalation compound.

where c takes the value 1 if there is a *Li*-ion on the lattice-site and 0 if not, r_{ij} is the distance between sites i and j lying on the same plane, r_m is the distance to the second neighbor (Fig. 1a) and $\in$ is the value of the attractive interaction at r_m. The out-of-plane interactions are the

interactions between ions that are located in different layers of graphite. These are modeled using the proposal of Derosa et al. [22]:

$$V_{ij} = c_i c_j \kappa \left(\frac{r_b}{r_{ij}}\right)^{\alpha} \tag{8}$$

here r_{ij} is the distance between the lattice-site i that is considered and another lattice-sites j out of plane of i, r_b is a distance scale factor, κ controls the repulsive interaction and α is a positive number used to regulate the range of the out-of-plane interactions. This type of power law appears in the Thomas-Fermi screening study of charge distribution in lamellar graphite intercalation compounds [32].

Experimentally, it is well known that in the insertion of *Li*-ions into graphite out-of-plane long-range interactions occur, which lead to the staging phenomenon [33,34,35]. The latter takes place in the intercalation process, where the ions completely fill some graphite layers leaving a constant number of empty graphite layers between any two filled layers. Fig. 1IV–I show stages IV, III, II and I, which are known to occur in the *Li*-graphite intercalation compounds. The out-of-plane long-range interactions are the result of the interactions of *Li*-ions with graphite [36,37,34] and they are not taken into account in the present theoretical model, which only considers short ranged repulsive interactions. Therefore, α is necessary to limit the out-of-plane interactions to the nearest planes where an isotropic interaction is appropriated to describe the transition of stage II to stage I that is observed in experiment.

On the basis of Eqs. (7) and (8) the Hamiltonian of the present system is:

$$H_0 = \sum_{i}^{N}\sum_{j\neq i}^{N_{ip}} \frac{c_i c_j \in}{2}\left[\left(\frac{r_m}{r_{ij}}\right)^{12} - 2\left(\frac{r_m}{r_{ij}}\right)^{6}\right] + \sum_{i}^{N}\sum_{j}^{N_{op}} \frac{c_i c_j \kappa}{2}\left(\frac{r_b}{r_{ij}}\right)^{\alpha} \tag{9}$$

where N, N_{ip} and N_{op} are the number of total, in-plane and out-of-plane lattice-sites respectively. As the interactions are pairwise it is necessary to include a factor of 1/2 in all the terms.

For the Monte Carlo simulations, a lattice of four layers of graphite is used. Each graphite layer consists of an arrangement of twelve by twelve lattice sites and periodic boundary conditions are used in the three dimensions. In this way we are assuming that the main contribution to lithium storage corresponds to the bulk part of the graphitic material, thus neglecting edge effects. To get values of intercalation entropy and enthalpy in the neighborhood of the phase transition, an extrapolation by means of rational functions [38] was performed.

4. Results and discussion

The $\in$ parameter of Eq. (7) is set to $\in = k_B T$ (where k_B is the Boltzman constant and T is the temperature) to represent an in-plane phase transition [39,40]. This means that there is an attractive interaction of value $k_B T$ between two inserted ions when they are separated by the in-plane distance $r_m = 4.26$ Å (Fig. 1a). For in-plane lattice distances lower than r_m or what is the same for the first neighbor in-plane lattice distance, Eq. (7) yields a very strong repulsion, thus limiting the maximum ion insertion number to one *Li*-ion for every six *C*-atoms (LiC_6).

The κ parameter of Eq. (8) is set to $\kappa = 10 k_B T$ and is used to control the difference between the chemical potentials of occurrence of stages I and II (see Fig. 2a). The α exponent of Eq. (8) is set to $\alpha = 4$ and is used to control the drop of the repulsive interactions and increase the steepness of the x vs. μ curve. Both values of κ and α are set to reproduce the transition of stage II to stage I in the experimental x vs. OCV curve. It is important to note that for *Li*-graphite intercalation compounds OCV and μ are equivalent ($\mu = -e_0 \mathrm{OCV}$). r_b in Eq. (8) is set equal to the distance of the $C-C$ chemical bond ($r_b = 1.42$ Å).

Fig. 2a shows in black the experimental x vs. OCV curve and in red the simulated one. By comparing these two curves it can be appreciated

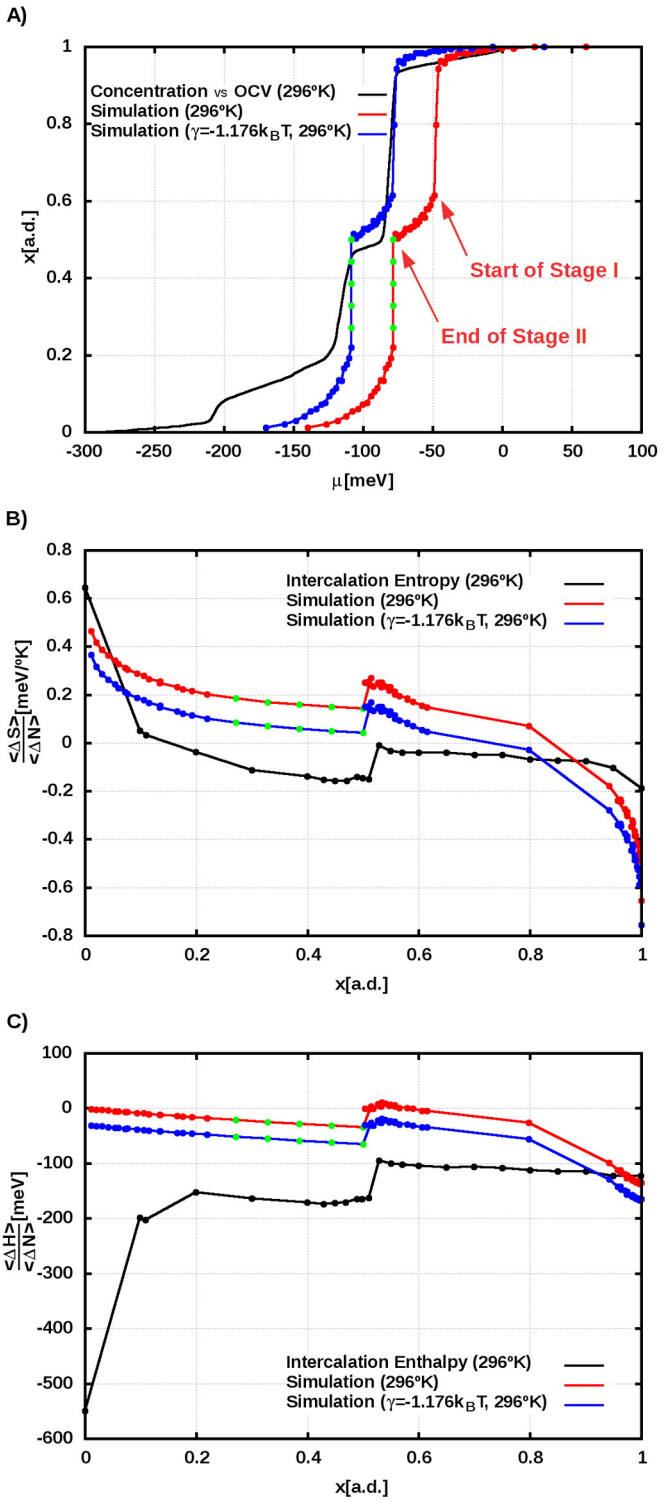

Fig. 2. A) Black: experimental *Li*-concentration (x) vs. chemical potential ($\mu = -e_0 \mathrm{OCV}$). Red and blue: simulated x vs. μ for Eqs. (9) and (10), respectively. Snapshots of a typical simulation run can be seen in the linked video. B) Black: experimental intercalation entropy vs. x. Red and blue: simulated intercalation entropy vs. x for Eqs. (9) and (10), respectively. B) Black: experimental intercalation enthalpy vs. x. Red and blue: simulated intercalation enthalpy vs. x for Eqs. (9) and (10), respectively. For all the cases $\gamma = -1.176 k_B T$ in Eq. (10).

a good correlation between them, in both raise and the energy difference between stages I and II. It can be also noted a shift of 30 meV between experimental and theoretical results. In this respect, the

simulated curve can be easily shifted by introducing an occupational term in the Hamiltonian as follows:

$$H = H_0 + \sum_i^N c_i \gamma \tag{10}$$

where c_i was already defined in Eq. (7) and $\gamma = -1.176 k_B T$. The blue curve in Fig. 2a corresponds to the shifted isotherm. Although the simulated curve is shifted with this choice, it does not reproduce the phase transition corresponding to less dense phases (stage III or higher), which appears experimentally around −200 meV (black curve in Fig. 2a). The later is due to the out-of-plane long-range interactions between ions and begin to be important below $x \approx 0.2$. They are beyond the scope of the present work, which is focused on the II–I transition.

Fig. 2b shows in black and blue the measured and simulated intercalation entropies respectively. As it can be appreciated, the main features of the experimental curve are well reproduced in the simulation. For $x \approx 0.5$ the experimental curve shows a step which is well reproduced both in position and magnitude by the simulated one. The step appears in the transition of stage II to stage I and it can be explained in the following way. Once stage II is completed, a new ion coming into graphite will find many empty sites with similar energies that may be occupied. These sites belong to empty sites of stage I and they are adding entropy to the system. It can be also noted that the experimental curve begins to be negative at $x \approx 0.2$ whereas the simulated one does not. This fact is due to the presence of the less dense phases (stage III or higher) in the experiment which are not included in the present theoretical model. The inclusion of long-range interaction required to get these less dense phases would lead to the use of a lower value of $\gamma < -1.176 k_B T$ in Eq. (10) and the simulated intercalation entropy would go down even more according to Eq. (6).

Fig. 2c shows in black and blue the experimental and simulated intercalation enthalpies respectively. At concentrations higher than $x \approx 0.2$ the shape of both curves agree very well. The step at $x \approx 0.5$ in the experimental curve is well reproduced in the simulated one. This step corresponds to an increment of the energy necessary to insert ions in the empty sites of stage I. The difference between the curve shapes at $x < 0.2$ may be attributed to the lack of the high order phases in the simulations. These high order phases may be also responsible for the lower ordinate position of the experimental curve with respect to the simulated one. However, it must be noted that the experimental curve includes the point $x = 0$.

Finally, at high concentrations ($x \approx 1$) the calculated intercalation entropy is lower in value than the experimental one as Fig. 2b shows. This fact could be attributed to vibrational entropy of the inserted ions that begins to be important at high ions concentrations. The extra energy result of this vibrational entropy would increase the experimental intercalation enthalpy at high ions concentration as Fig. 2c shows.

5. Conclusions

In the present article we have developed a theoretical approach to determine the intercalation entropy and enthalpy of electrochemical intercalation compounds. Within the present approximation, the system has been modeled as a lattice-gas. Particularly, the *Li*-graphite intercalation compound has been analyzed. To reproduce the staging phenomenon present in this type of intercalation compounds, the interactions between ions were divided into in-plane and out-of-plane ones. The in-plane interactions were modeled by an attractive Lenard-Jones potential and the out-of-plane interactions were modeled as a repulsive power-law decay. By using grand canonical Monte Carlo simulations the intercalation entropy and enthalpy were determined and a very good correlation with the experimental measurements was obtained. Although vibrational effects are absent in the present modeling, the main features of the experimental intercalation entropy and enthalpy were well reproduced. A further refinement of the interaction potential would be valuable to reproduce the low density phases of lithium intercalation in graphite. Additionally, the grand canonical simulation could be implemented within an atomistic model of the system including atomic vibrational motion. This would allow to consider the vibrational entropy contribution.

Supplementary data to this article can be found online at http://dx.doi.org/10.1016/j.elecom.2016.02.003.

Acknowledgements

National Council of Scientific and Technological Research of Argentina (CONICET), SECyT-Universidad Nacional de Córdoba, and No. PME 2006-01581 for financial support. CONICET-PIP No. 11220110100992 and Program BID (No. PICT 2012-2324), for computational tools.

References

[1] Y. Reynier, R. Yazami, B. Fultz, The entropy and enthalpy of lithium intercalation into graphite, J. Power Sources 119–121 (2003) 850–855.
[2] Y.F. Reynier, R. Yazami, B. Fultz, Thermodynamics of lithium intercalation into graphites and disordered carbons, J. Electrochem. Soc. 151 (3) (2004) A422–A426.
[3] S.R. Cain, W. Infantolino, A. Anderson, E. Tasillo, P. Wolfgramm, Thermochemistry and equilibration time scales for a rechargeable lithium ion battery, Electrochim. Acta 185 (2015) 250–258.
[4] H. Yang, J. Prakash, Determination of the reversible and irreversible heats of a $LiNi_{0.8}Co_{0.15}Al_{0.05}O_2$/natural graphite cell using electrochemical calorimetric technique, J. Electrochem. Soc. 151 (8) (2004) A1222–A1229.
[5] P.J. Osswald, M. del Rosario, J. Garche, A. Jossen, H.E. Hoster, Fast and accurate measurement of entropy profiles of commercial lithium-ion cells, Electrochim. Acta 177 (2015) 270–276.
[6] J.P. Schmidt, A. Weber, E. Ivers-Tiffée, A novel and precise measuring method for the entropy of lithium-ion cells: ΔS via electrothermal impedance spectroscopy, Electrochim. Acta 137 (2014) 311–319.
[7] K. Onda, T. Ohshima, M. Nakayama, K. Fukuda, T. Araki, Thermal behavior of small lithium-ion battery during rapid charge and discharge cycles, J. Power Sources 158 (1) (2006) 535–542.
[8] S. Abada, G. Marlair, A. Lecocq, M. Petit, V. Sauvant-Moynot, F. Huet, Safety focused modeling of lithium-ion batteries: a review, J. Power Sources 306 (2016) 178–192.
[9] V.V. Viswanathan, D. Choi, D. Wang, W. Xu, S. Towne, R.E. Williford, J.-G. Zhang, J. Liu, Z. Yang, Effect of entropy change of lithium intercalation in cathodes and anodes on Li-ion battery thermal management, J. Power Sources 195 (11) (2010) 3720–3729.
[10] J. Hong, H. Maleki, S. Al Hallaj, L. Redey, J.R. Selman, Electrochemical-calorimetric studies of lithium-ion cells, J. Electrochem. Soc. 145 (5) (1998) 1489–1501.
[11] C. Heubner, M. Schneider, C. Lämmel, A. Michaelis, Local heat generation in a single stack lithium ion battery cell, Electrochim. Acta 186 (2015) 404–412.
[12] M.K. Aydinol, A.F. Kohan, G. Ceder, K. Cho, J. Joannopoulos, *Ab initio* study of lithium intercalation in metal oxides and metal dichalcogenides, Phys. Rev. B 56 (1997) 1354–1365.
[13] M.K. Aydinol, G. Ceder, First-principles prediction of insertion potentials in Li–Mn oxides for secondary Li batteries, J. Electrochem. Soc. 144 (11) (1997) 3832–3835.
[14] D. Datta, J. Li, N. Koratkar, V.B. Shenoy, Enhanced lithiation in defective graphene, Carbon 80 (2014) 305–310.
[15] C. Robledo, M. Otero, G. Luque, O. Cámara, D. Barraco, M. Rojas, E. Leiva, First-principles studies of lithium storage in reduced graphite oxide, Electrochim. Acta 140 (2014) 232–237.
[16] P. Ganesh, J. Kim, C. Park, M. Yoon, F.A. Reboredo, P.R.C. Kent, Binding and diffusion of lithium in graphite: quantum Monte Carlo benchmarks and validation of Van der Waals density functional methods, J. Chem. Theory Comput. 10 (12) (2014) 5318–5323.
[17] E. Mostaani, N.D. Drummond, V.I. Fal'ko, Quantum Monte Carlo calculation of the binding energy of bilayer graphene, Phys. Rev. Lett. 115 (2015) 115501.
[18] Z.E. Hughes, T.R. Walsh, Computational chemistry for graphene-based energy applications: progress and challenges, Nanoscale 7 (2015) 6883–6908.
[19] D.T. Kulp, S.H. Garofalini, Molecular dynamics studies of lithium injection in model cathode/electrolyte systems, J. Electrochem. Soc. 143 (7) (1996) 2211–2219.
[20] S. Garofalini, P. Shadwell, Molecular dynamics simulations of cathode/glass interface behavior: effect of orientation on phase transformation, Li migration, and interface relaxation, J. Power Sources 89 (2) (2000) 190–200.
[21] C.M. Shumeyko, E.B.W. III, A molecular dynamics study of lithium grain boundary intercalation in graphite, Scr. Mater. 102 (2015) 43–46.
[22] P.A. Derosa, P.B. Balbuena, A lattice-gas model study of lithium intercalation in graphite, J. Electrochem. Soc. 146 (10) (1999) 3630–3638.
[23] T. Zheng, J.R. Dahn, Lattice-gas model to understand voltage profiles of $LiNi_xMn_{2-x}O_4$/Li electrochemical cells, Phys. Rev. B 56 (1997) 3800–3805.
[24] M. Landstorfer, T. Jacob, Mathematical modeling of intercalation batteries at the cell level and beyond, Chem. Soc. Rev. 42 (2013) 3234–3252.
[25] A.A. Franco, Multiscale modelling and numerical simulation of rechargeable lithium ion batteries: concepts, methods and challenges, RSC Adv. 3 (2013) 13027–13058.
[26] A. Latz, J. Zausch, Multiscale modeling of lithium ion batteries: thermal aspects, Beilstein J. Nanotechnol. 6 (2015) 987–1007.

[27] S.P. Kelty, C.M. Lieber, Atomic-resolution scanning-tunneling-microscopy investigations of alkali-metal — graphite intercalation compounds, Phys. Rev. B 40 (1989) 5856–5859.
[28] J.-C. Charlier, X. Gonze, J.-P. Michenaud, First-principles study of the stacking effect on the electronic properties of graphite(s), Carbon 32 (2) (1994) 289–299.
[29] Z.Y. Rong, P. Kuiper, Electronic effects in scanning tunneling microscopy: Moiré pattern on a graphite surface, Phys. Rev. B 48 (1993) 17427–17431.
[30] J.E. Lennard-Jones, Cohesion, Proc. Phys. Soc. 43 (5) (1931) 461.
[31] J.-P. Hansen, L. Verlet, Phase transitions of the Lennard-Jones system, Phys. Rev. 184 (1969) 151–161.
[32] L. Pietronero, S. Strässler, H.R. Zeller, M.J. Rice, Charge distribution in *c* direction in lamellar graphite acceptor intercalation compounds, Phys. Rev. Lett. 41 (1978) 763–767.
[33] T. Ohzuku, Y. Iwakoshi, K. Sawai, Formation of lithium–graphite intercalation compounds in nonaqueous electrolytes and their application as a negative electrode for a lithium ion (shuttlecock) cell, J. Electrochem. Soc. 140 (9) (1993) 2490–2498.
[34] A.M. Dimiev, G. Ceriotti, N. Behabtu, D. Zakhidov, M. Pasquali, R. Saito, J.M. Tour, Direct real-time monitoring of stage transitions in graphite intercalation compounds, ACS Nano 7 (3) (2013) 2773–2780.
[35] C. Sole, N.E. Drewett, L.J. Hardwick, In situ Raman study of lithium-ion intercalation into microcrystalline graphite, Faraday Discuss. 172 (2014) 223–237.
[36] S.A. Safran, D.R. Hamann, Long-range elastic interactions and staging in graphite intercalation compounds, Phys. Rev. Lett. 42 (1979) 1410–1413.
[37] M.S. Dresselhaus, G. Dresselhaus, Intercalation compounds of graphite, Adv. Phys. 51 (1) (2002) 1–186.
[38] W.H. Press, S.A. Teukolsky, W.T. Vetterling, B.P. Flannery, Numerical Recipes In C, 2Cambridge university press, Cambridge, 1996.
[39] R.J. Baxter, Hard hexagons: exact solution, J. Phys. A Math. Gen. 13 (3) (1980) L61.
[40] R.J. Baxter, Exactly Solved Models in Statistical Mechanics, Courier Corporation, 2007.